Quaternary Research 85 (2016) 107–117

Contents lists available at ScienceDirect

Quaternary Research

journal homepage: www.elsevier.com/locate/yqres

Rapid thinning of the Welsh Ice Cap at 20–19 ka based on ^{10}Be ages

Philip D. Hughes [a,*], Neil F. Glasser [b], David Fink [c]

[a] Geography, School of Environment, Education and Development, University of Manchester, Manchester M13 9PL, England, UK
[b] Department of Geography and Earth Sciences, Aberystwyth University, Aberystwyth SY23 3DB, Wales, UK
[c] Australian Nuclear Science and Technology Organisation, PMB1, Menai, NSW 2234, Australia

ARTICLE INFO

Article history:
Received 3 June 2015
Available online 8 January 2016

Keywords:
Welsh Ice Cap
Nunatak
10Be
Cosmogenic exposure dating
Rhinogs
Moelwyns
Arenigs
Deglaciation

ABSTRACT

New ^{10}Be ages from the summits of three mountain areas of North Wales reveal a very similar exposure timing as the Welsh Ice Cap thinned after the global Last Glacial Maximum. Eight bedrock and one boulder sample gave a combined arithmetic mean exposure age of 19.08 ± 0.80 ka (4.2%, 1σ). Similar exposure ages over a 320 m vertical range (824 to 581 m altitude) show that ice cap thinning was very rapid and spatially uniform. Using the same production rate and scaling scheme, we recalculated six published ^{10}Be exposure ages from the nearby Arans, which also covered a similar elevation range from 608 to 901 m and obtained an arithmetic mean of 19.41 ± 1.45 ka (7.5%, 1σ). The average exposure age of all 15 accepted deglaciation ages is 19.21 ± 1.07 (5.6%, 1σ). The complete dataset from North Wales provides very strong evidence indicating that these summits became exposed as nunataks at 20–19 ka. This result provides important insight to the magnitude of ice surface lowering and behavior of the Welsh Ice Cap during the last deglaciation that can be compared to other ice masses that made up the British-Irish Ice Sheet.

Introduction

The Welsh Ice Cap has been the subject of research for over 150 yr. While the exact location of the ice divide varies in the literature, it is clear that the thickest part of the Late Pleistocene Welsh Ice Cap was positioned over the Arenig Mountains in North Wales (Fearnsides, 1905; Rowlands, 1979), with an ice thickness of >1000 m submerging even the highest summits. From the Arenigs, ice flowed westward from these areas toward the Cardigan Bay (Foster, 1970a,b) and eastward toward the borderlands of England (Travis, 1944) — see Figure 1 for locations. Afterward the summits emerged from below a thinning ice cap and valley glaciers formed local moraines (Rowlands, 1979). The last phase of glaciation in North Wales occurred during the Younger Dryas (12.9–11.7 ka) when cirque glaciers were present (Hughes, 2002a, 2009; Bendle and Glasser, 2012).

Although the Welsh Ice Cap was largely independent of the British-Irish Ice Sheet, which had its thickest centers over Ireland, England and Scotland, there were some incursions of Irish Sea ice into Wales, such as in the Vale of Clwyd (Rowlands, 1971) and across Anglesey and the Lleyn Peninsula (Thomas and Chiverrell, 2007). In north Wales the British-Irish Ice Sheet subsumed the Welsh Ice Cap (Clark et al., 2012) while in mid and south Wales the Welsh Ice Cap did not coalesce with the British-Irish Ice Sheet. The timing of retreat of the various sectors of the British-Irish Ice Sheet has been the subject of intense research (e.g. Ballantyne, 2010; Chiverrell et al., 2013; Everest et al., 2013). However, the history of the Welsh Ice Cap has not been the focus of recent geochronological investigations despite there being very little known about the timing of ice cap retreat. Most of the geochronology for the last Welsh Ice Cap is based on dating the retreat of ice margins (see Hughes et al., 2011 for a review of ages for both the Welsh Ice Cap and the British-Irish Ice Sheet) with only one study by Glasser et al. (2012) providing constraints on the timing of vertical changes in the former ice cap. Despite the lack of dating control, the geomorphology of the landscape produced by the last Welsh Ice Cap is well understood (e.g. Jansson and Glasser, 2005). This geomorphological evidence has provided the basis for recent modeling simulations (e.g. Patton et al., 2013a, 2013b).

Glasser et al. (2012) provided eight paired ^{26}Al/^{10}Be exposure ages from the Aran mountain summits in Wales in order to establish the vertical exposure history of the Welsh Ice Cap. This study aimed to test both the timing of exposure and whether there was any evidence of complex exposure history. The results indicated that the summits were exposed at c. 20–17 ka (subject to recalculation using new production rates in this paper) and that there was no evidence of complex exposure history. Six out of the eight exposure ages overlapped within error suggesting near complete zeroing of the cosmogenic nuclide signal by prior glaciation and a simple exposure history following ice retreat. Two samples were old outliers and suggest inheritance and localized patches of reduced erosion on the summit ridge. The exposure history of the Aran summits is consistent with the thinning of the Welsh Ice Cap soon after Heinrich Event 2, which Hughes and Gibbard (2015) argue terminated the global last glacial maximum (LGM). However, in order to

* Corresponding author.
E-mail address: philip.hughes@manchester.ac.uk (P.D. Hughes).

http://dx.doi.org/10.1016/j.yqres.2015.11.003
0033-5894/

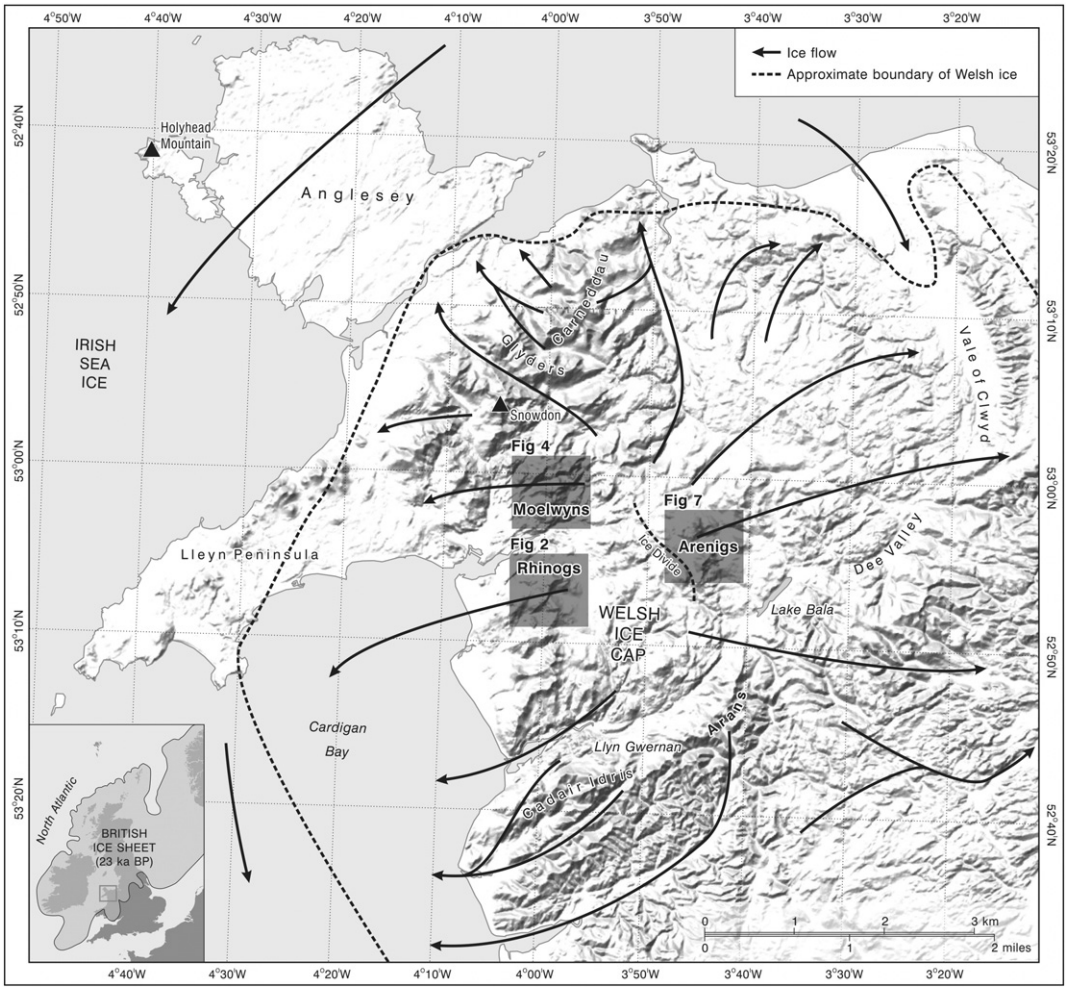

Figure 1. Location map of the field areas and sample sites denoted by gray shaded squares. The ice flow directions are primarily based on field observations in this study and also evidence presented by Smith and George (1961), Foster (1970b), Whittow and Ball (1970), Rowlands (1979), Addison (1997), Jansson and Glasser (2005), Glasser et al. (2012) and Patton et al. (2013a,b). The ice divide in the Arenig area is based on Rowlands (1979). In some areas the ice flow patterns are disputed, such as in the Snowdon–Glyders area (see McCarroll and Ballantyne, 2000) but the general patterns indicated above are agreed by most workers.

achieve a regional picture of ice cap thinning, exposure ages are needed from a wider area in order to test whether ice cap thinning occurred locally or regionally soon after Heinrich Event 2. Furthermore, new exposure ages are calculated using revised production rates from Ballantyne and Stone (2012), with previously published ages such as those from the Arans (Glasser et al., 2012) recalculated accordingly.

This paper presents evidence from three mountain ranges in central Snowdonia, North Wales: the northern Rhinogs, the Moelwyns and the Arenigs (Fig. 1). The northern Rhinogs culminate at Moel Ysgyfarnogod (623 m), the Moelwyns at Moelwyn Mawr (770 m) and the Arenigs at Arenig Fawr (854 m). The mountains are strategically important for understanding ice cap dynamics because these areas were close to the thickest center of the last Welsh Ice Cap (Fearnsides, 1905; Greenly, 1919; Foster, 1968, 1970a,b; Addison, 1997; Jansson and Glasser, 2005; Glasser et al., 2012; Patton et al., 2013a,b). Terrestrial cosmogenic nuclide exposure ages have never been published from these three sites. This study exploits the quartz-rich lithologies of these areas to provide a new cosmogenic exposure chronology for the mountain summits. The primary aim is to establish the exposure ages of the summits of the northern Rhinogs, the Moelwyns and the Arenigs and compare this with the recently-obtained paired $^{26}Al/^{10}Be$ exposure ages from the nearby Arans (Glasser et al., 2012). This will provide a time constraint for understanding the vertical thinning of the last Welsh Ice Cap at the end of the last cold stage. In addition, the timing of ice cap thinning over Wales will also provide an interesting comparison with deglaciation geochronologies from the wider British-Irish Ice Sheet (e.g. Chiverrell et al., 2013; Ballantyne and Stone, 2015).

Study area

The study area spans a narrow latitudinal and longitudinal range from 52.8763 to 52.9819°N and 4.0013 to 3.7432° W. The Rhinogs are formed in the Cambrian sandstones and mudstones of the Rhinog Formation and sandstones of the Hafotty Formation. The latter rock type forms the summit areas of most of the northern Rhinogs. Ordovician microgabbro intrusions also occur in this area emplaced into the Cambrian rocks. The Moelwyns are formed in Ordovician siltstones (slates) and volcanics. We targeted quartz veins which are widely found in both. The volcanics comprise an unnamed intrusive rhyolite and tuffite of the Moelwyn Volcanic Formation. The Arenigs are formed in Ordovician volcanics dominated by felsic tuffs and quartz–latite intrusions. The tuffs form the summit ridges with tuffs of the Aran Fawddwy Formation predominant with a small area of tuffs belonging to the Benglog Volcanic Formation. All geological terminologies for these areas were obtained from EDINA Geology Digimap (2014).

https://doi.org/10.1016/j.yqres.2015.11.003 Published online by Cambridge University Press

Methods

Geomorphology

This project focused on the evidence of glaciation on the summits of the Rhinogs, Moelwyns and Arenigs. Glacial erosional features are widely evident, such as striations, roches moutonnées, whalebacks and rock pavements, and these were targeted for cosmogenic dating. Perched boulders resting on ice-polished bedrock were also noted as evidence of ice overriding summits. The main focus of the project was to establish the exposure history of the summits of the three mountain areas. Thus, samples were taken from rock surfaces at or close to the apex of the watersheds in these mountain areas. Regional patterns of ice flows were established using topographic maps and satellite imagery as well as utilizing field evidence from a number of previous research studies (e.g. Foster, 1970b; Rowlands, 1979).

Geochronology

Eight samples were taken from ice-scoured striated bedrock on the summit watersheds of the northern Rhinogs (1 sandstone and 1 quartz-vein sample), Moelwyns (3 quartz vein samples) and Arenigs (3 quartz vein samples). Glacially-abraded surfaces can yield reliable exposure ages when erosion by ice from the most recent ice advance has been sufficient to remove the accumulated in-situ cosmogenic signal from all previous exposures. This has been shown to be a reliable approach (Dielforder and Hetzel, 2014) and has been applied in areas of the British Isles (e.g. McCormack et al., 2011; Rolfe et al., 2012). However, bedrock is often overlooked in favor of boulders since the prevailing pattern of sampling favors erratics on the assumption that transported erratics are more likely to have minimal inheritance and there is no way of detecting inheritance prior to sampling (Balco, 2011). The expansive ice-overridden summit regions in this work are characterized by exposed, gently sloping polished bedrock sheets on which are perched erratics and cobbles of various sizes. Unlike the short transit times for boulders in typical alpine glacial systems prior to deposition at terminal moraine locations, the erratics on these open summit bedrock watersheds may well have resided sub-aerially for a considerable period prior to ice cap thinning and final glacial retreat. Hence it was not *a priori* assumed that erratics would provide the best target and one glacially-transported boulder was also sampled (sandstone) immediately adjacent to a bedrock sample (quartz vein) in the Rhinogs to form a bedrock–boulder pair. Details of all 9 samples are provided in Table 1.

Samples were crushed, sieved and cleaned with aqua regia at the University of Manchester Geography Laboratories. The 250–500 μm fraction (~100–200 g) was added to 1 L glass beakers, mixed with aqua regia [60 ml of conc. HNO_3 and 180 ml of conc. HCl], then left to stand for 24 h and stirred twice in this period. The aqua regia was then decanted and replaced until the solution was clear (1–2 washes). After the aqua regia treatment the sample was rinsed with water (~6 times, wash and decant), then 100–200 ml of NaOH was added, stirred, then left for 2–4 h. The samples were then washed with water and dried. The samples were then sent for further preparation and AMS measurement at the Cosmogenic Geochemistry Laboratories at the Australian Nuclear Science and Technology Organisation (ANSTO). Here, quartz separation and purification were achieved by hot phosphoric acid etching (Mifsud et al., 2013) and elution of the ^{10}Be fraction (Child et al., 2000). Instead of selective hydrofluoric acid etching to separate quartz (Kohl and Nishiizumi, 1992) repeated treatments of hot ortho-phosphoric acid (H_3PO_4 85% w/w) at 250°C were used to remove non-quartz mineral species followed by one or two cycles of HF (2%) etch. The hot H_3PO_4 method does not attack quartz as severely as HF, making it preferable when the quartz grain size is very small, such as in silcretes, chert and other quasi-amorphous silicates or when the quartz concentration in the bulk is very low. The samples were all quartz-rich and the initial rock masses used for processing (in the 250–500 μm fraction) ranged from ~100 to 200 g, with yields of about 40%–95% of acceptable quartz following the treatment described above. Following quartz dissolution in 50% w/w HF and an addition of a ^{9}Be carrier (~0.32 mg) all samples were carefully fumed with the addition of 5 ml of $HClO_4$. Dowex anion and cation resins (1X-8 and 50W-X8) were used for ion chromatography separation to eliminate matrix contaminations (Fe, Ca, Ti, etc.). Following pH-adjustment $Be(OH)_2$ was precipitated, carefully dried and calcined at 800°C. The final BeO material (0.5 to 1.0 mg oxide) was mixed with a Nb binder (BeO: Nb = 1:4) (Fink et al., 2000) and then pressed into target cathodes for AMS measurement.

AMS targets were measured for ^{10}Be at the ANTARES AMS Facility at ANSTO (Fink and Smith, 2007). $^{10}Be/^{9}Be$ ratios (see Table 2) were normalized against the NIST-4325 standard reference material ($^{10}Be/^{9}Be$ ratio of $27{,}900 \times 10^{-15}$). All isotopic ratios were corrected using full chemistry procedural blanks prepared from dissolved and purified beryl crystal with a measured $^{10}Be/^{9}Be$ ratio of $5.66 \pm 0.62 \times 10^{-15}$ ($n = 4$, 2 targets) and with a ^{9}Be concentration of 1080 ± 11 ug/g. Background corrections ranged between 1.7% and 2.8% of the measured AMS $^{10}Be/^{9}Be$ ratio (Table 1). Repeat measurements of individual samples were combined as weighted means with the larger of the mean standard error or total statistical error. Final analytical errors in the ^{10}Be

Table 1
Sample information, AMS cosmogenic $^{10}Be/^{9}Be$ results and analytical errors.

Sample name	Alt (m)	Latitude (N)	Longitude (W)	Quartz mass (g)	^{9}Be spike mass[a] (mg)	$^{10}Be/^{9}Be$ ($\times 10^{-15}$)[b]	$^{10}Be/^{9}Be$ error (%)	Sample thickness (cm)	Horizon shielding correction[c]	Thickness correction[c]
Rhinogs										
RH-01	589	52.8763	−4.0013	80.511	0.321	535.4	2.65	3	1.000	0.975
RH-02	581	52.8889	−3.9970	87.317	0.321	602.8	2.11	3	1.000	0.975
RH-03[d]	581	52.8887	−3.9971	90.041	0.320	539.8	1.74	5	1.000	0.959
Moelwyns										
MW-01	700	52.9748	−3.9941	91.752	0.323	658.1	2.54	5	1.000	0.959
MW-02	650	52.9792	−3.9973	90.209	0.325	591.5	2.30	5	0.960	0.959
MW-03	670	52.9819	−3.9987	90.254	0.325	627.5	2.36	5	1.000	0.959
Arenigs										
ARENIG-01	680	52.9585	−3.7569	70.569	0.324	469.3	2.77	5	1.000	0.959
ARENIG-02	655	52.9590	−3.7538	47.079	0.325	304.2	2.70	3	1.000	0.975
ARENIG-03	824	52.9185	−3.7432	90.271	0.326	719.1	2.29	4	1.000	0.967

[a] ^{9}Be spike mass from beryl crystal solution prepared at the ANSTO Cosmogenic Laboratory with 1080 ± 11 μg $^{9}Be/g$ solution.
[b] Final AMS $^{10}Be/^{9}Be$ ratio from weighted mean of repeat measurements. All AMS ratios were corrected for full chemistry procedural blank and calibrated against NIST-4325 AMS $^{10}Be/^{9}Be$ standard reference material with a nominal value of $27{,}900 \times 10^{-15}$. Beryl chemistry $^{10}Be/^{9}Be$ blank (2 cathodes, $n = 4$) of $(5.66 \pm 0.62) \times 10^{-15}$.
[c] Horizon shielding calculated using $m = 2.65$; thickness correction using a rock density of 2.7 g/cm^3 and $\Lambda = 150$ g/cm^2.
[d] All samples are from bedrock quartz veins apart from RH03, a boulder of dimension 2.5 × 1.8 m and 1.2 m in height.

https://doi.org/10.1016/j.yqres.2015.11.003 Published online by Cambridge University Press

Table 2
^{10}Be cosmogenic concentrations and calculated exposure ages.

Sample name	Alt (m)	^{10}Be conc. & analytical error (atoms/gram) ($\times 10^3$)[a]	Scaling factor[b]	Total site production rate (atoms/g/y)[c]	^{10}Be exposure age (ka)	Exposure age error (absolute) (ka)	Exposure age error (analytical) (ka)
Rhinogs							
RH-01	589	142.6 (4.9)	1.761	7.3911	19.39	0.97	0.69
RH-02	581	147.9 (4.5)	1.748	7.340	20.26	0.96	0.64
RH-03[d]	581	128.4 (3.6)	1.748	7.218	17.86	0.81	0.52
Arith mean (RH01,02 only) ($\pm 1\sigma$) = 19.82 ± 0.62 (3.1%) ka. Reduced χ^2 = 0.9							
Moelwyns							
MW-01	700	154.9 (5.2)	1.938	8.002	19.45	0.94	0.66
MW-02	650	142.3 (4.6)	1.857	7.359	19.43	0.88	0.60
MW-03	670	151.0 (4.9)	1.889	7.799	19.46	0.93	0.64
Arith mean (± SME) = 19.45 ± 0.4 (2.1%) ka. Reduced $\chi^2 < 1$							
Arenigs							
ARENIG-01	680	144.2 (5.1)	1.905	7.866	18.41	0.92	0.66
ARENIG-02	655	140.3 (4.9)	1.865	7.828	18.00	0.90	0.64
ARENIG-03	824	173.2 (5.5)	2.153	8.963	19.42	0.93	0.63
Arith mean ($\pm 1\sigma$) = 18.61 ± 0.7 (3.9%) ka. Reduced χ^2 = 1.4							
Arans (*recalculated from* Glasser et al., 2012)							
AB-01	878	175.2 (6.4)	2.252	9.453	18.62	0.95	0.69
AB-06	608	145.5 (6.7)	1.790	7.513	19.46	1.13	0.90
AF-01	818	168.2 (6.4)	2.142	9.065	18.64	0.98	0.72
AF-02	880	195.1 (7.2)	2.256	9.236	21.24	1.07	0.78
AF-03	901	197.9 (7.7)	2.296	9.479	20.99	1.09	0.81
AF-04	638	133.5 (6.1)	1.837	7.647	17.53	1.00	0.80
Arith mean ($\pm 1\sigma$) = 19.41 ± 1.45 (7.5%) ka. Reduced χ^2 = 3nn5							

[a] ^{10}Be concentration derived from final mean ^{10}Be/^{9}Be ratio (see Table 1). Total analytical error in ^{10}Be concentration based on final AMS ^{10}Be/^{9}Be error, 1% error ion ^{9}Be spike value and 2% reproducibility error based on the standard deviation from long term repeat measure of the NIST-4325 primary standard.
[b] Total spallation and muon scaling factor for sample site and normalized to sea-level and high latitude derived using the same formalism as from Stone (2000).
[c] Site production rate based on a reference sea-level high latitude spallation production rate from Chiverrell et al. (2013) of 4.20 ± 0.15 ^{10}Be atoms/g/y (see text) and an assumed total SLHL muon contribution of 0.11 at/g/y scaled independently as described by Stone (2000) and corrected for shielding and sample thickness as given in Table 1 (and Glasser et al., 2012 for the Arans).
[d] Boulder sample not included in bedrock averaging.

concentration (^{10}Be/g-quartz) were derived from the quadrature addition of the 1σ spread in repeat measure of AMS standards (1.5%), final statistical error in the AMS ratio, and a 1% error in Be-spike assay resulting in a combined analytical error ranging from 2.8% to 3.6% (Table 2). Site spallation and muon production rates were scaled independently from sea-level and high latitude (SLHL) following the prescription given by Stone (2000). A range of reference production rates (i.e. rates defined for SLHL) can be used to calculate exposure ages and there remain uncertainties over suitable values for Wales. In order to compare with other published data, we adopt the same ^{10}Be reference production rate used for west Wales and the Irish Sea area by Chiverrell et al. (2013) of 4.20 ± 3.6% atoms g^{-1} a^{-1} based on a calibrated dataset from northwest Scotland (Ballantyne and Stone, 2012). We choose a SLHL surface ^{10}Be muon total production rate of 0.1 at/g/y (i.e. ~2.5% of total production (Stone, 2000) (see Table 2) and a ^{10}Be decay constant of 4.99×10^{-7} a^{-1}, based on the half-life value of 1.387 ± 0.012 Ma (Chmeleff et al., 2010; Korschinek et al., 2010). Glasser et al. (2012) have previously published ^{10}Be ages from the neighboring Arans and to enable a direct comparison, we have recalculated these ages using identical methods as described above.

Reduced paleo-geomagnetic dipole strengths result in increased time-integrated production rates compared to present day (or early Holocene) estimates. Hence apparent exposure ages based on a non-varying geomagnetic field intensity (i.e. constant site production rate) usually will overestimate the true age. For this study, at the high northern latitude of ~52°N, production rate corrections for a time varying geomagnetic field become marginal and also rather insensitive to choice in scaling or palaeomagnetic record. Direct comparison of age calculations based on Dunai scaling with a time varying geomagnetic field (Dunai, 2002) results in ages <1% younger than those based on time invariant Dunai calculations. Corrections to site specific production rates due to horizon topographic shielding of cosmic rays were negligible apart from one sample (MW02; 0.96) whereas corrections for sample thicknesses (~3–5 cm) ranged from ~0.95 to 0.97 (thickness corrections were carried out by integrating the effective cosmic ray flux over the given depth using $\Lambda = 150$ g/cm^2 and $\rho = 2.7$ g/cm^3). Corrections for seasonal snow cover were not included as we believe that little summer snow accumulates due to the open and flat expanses of the bedrock summits. Age correction due to surface weathering becomes progressively more important with increasing zero-erosion minimum age. For example, a reasonable erosion rate of 1 mm/ka for quartz vein samples would amount to <0.5 ka increase in age over a 20 ka exposure period. Hence with the above uncertainties, choice in relative muon production contribution (see Braucher et al., 2013) and scaling schemes (Balco et al., 2008), our conclusions regarding the exposure age determinations for these Welsh summits are not altered.

Geomorphology

Geomorphology — Rhinogs

The northern Rhinogs contain extensive rock pavements, striated whalebacks and roches moutonnées with several small glacial lakes occupying bedrock hollows on the watershed (Fig. 2). The rock pavements are littered with perched boulders. The sandstone rocks are heavily fractured in this area and perched rocks appear to have been plucked off bedding planes and then transported up to several hundreds of meters. While local in origin the boulders are often subrounded or subangular and display evidence of significant glacial abrasion. Striations were recorded on the bedrock at the sample sites (see Fig. 3) and have an east-west lineation (85/265 to 110/290°) which is consistent with ice movement from the east (Foster, 1970b) (Fig. 2).

https://doi.org/10.1016/j.yqres.2015.11.003 Published online by Cambridge University Press

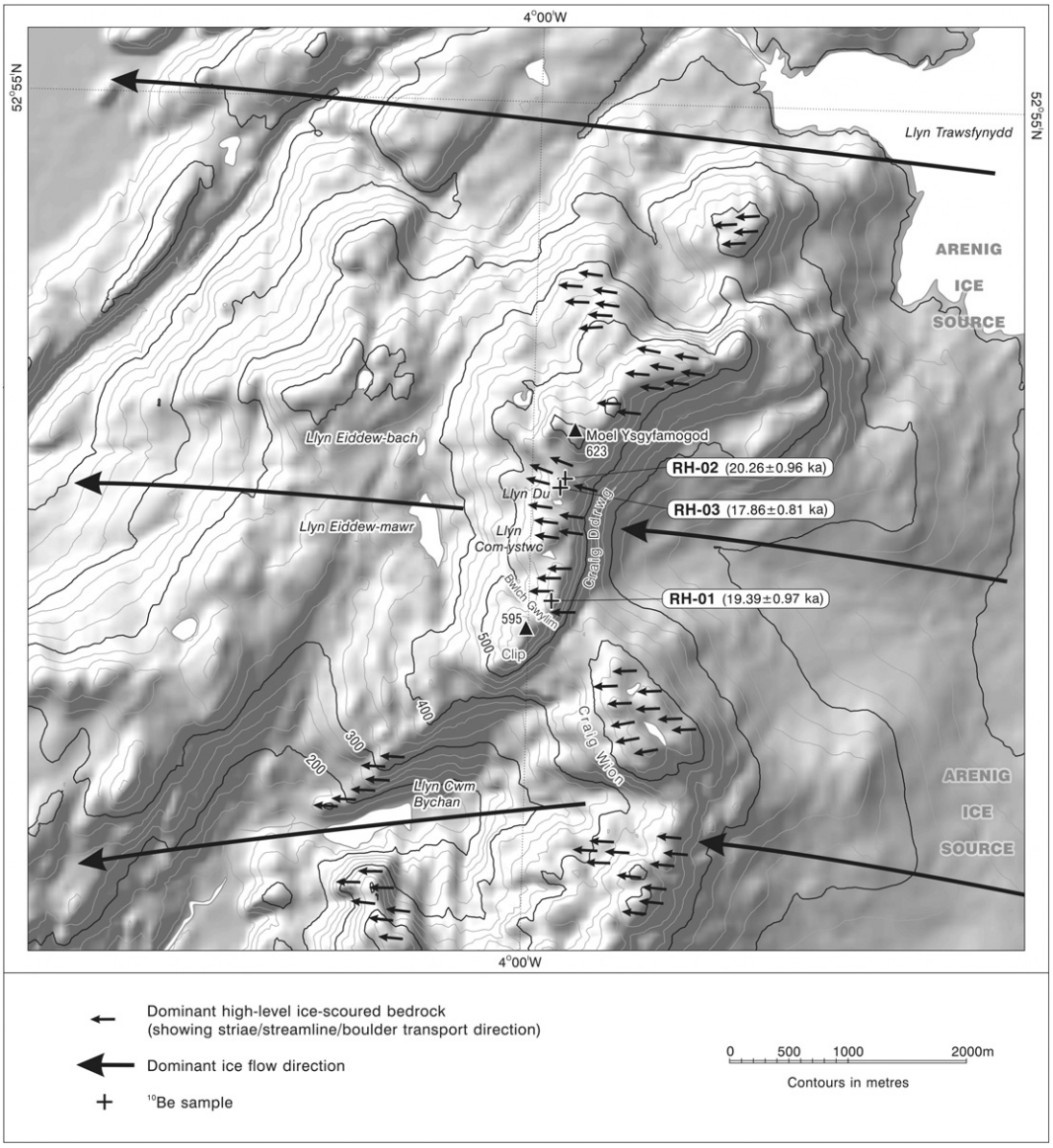

Figure 2. The Rhinogs showing the main ice flow directions and sample sites for ^{10}Be exposure dating. Location is marked on Figure 1. For all Figures 2–8, exposure age errors are calculated as absolute by quadrature inclusion of a 3.6% production rate error with the stated analytical errors given in Table 2.

Geomorphology — Moelwyns

The southern summit area of Moelwyn Bach (710 m) is characterized by extensive rock pavements, formed in the tuffite of the Moelwyn Volcanic Formation, with occasional perched boulders of local origin. The northern (and highest) summit area is formed in metamorphosed siltstones (slates) (Nant Ffrancon Subgroup) with quartz veins. Again these slates form smoothed pavements, whalebacks and roches moutonnées. All of these rock features exhibit features (such as streamlining, local boulders plucked from bedrock joints, grooves and occasional striae on the finer grained siltstones) consistent with ice scouring from the east to the west (Fig. 4).

To the north of Moelwyn Bach the ridge of Craigysgafn leads on to Moelwyn Mawr (770 m) (Figs. 4 and 5). This ridge is formed in rhyolite and tuffite with numerous quartz veins, and in some cases extensive quartz outcrops (Fig. 6). The rocks of this ridge are smoothed with numerous whalebacks and roches moutonnées. As with the summit of Moelwyn Bach this is consistent with ice scouring. The glacially-eroded features on Craigysgafn are aligned east–west. However, the eastern face of Craigysgafn is the steeper face (Figs. 4 and 5), although this is not indicative of ice direction over the ridge (i.e. through lee-side plucking). Instead, this steeper eastern face is the result of localized glaciation in Cwm Stwlan after the ridge top was abraded by ice — probably during the Younger Dryas since moraines are present in this cwm (partly concealed by the raised hydroelectric lake level).

Geomorphology — Arenigs

The summit ridge of Arenig Fawr (Fig. 7) is characterized by bare rock surfaces formed in volcanic tuffs with occasional quartz veins. Evidence of glacier abrasion is best displayed in the north near Simdde Ddu (697 m a.s.l.). Further south toward the higher peak of Arenig Fawr (854 m a.s.l.) the bedrock surface is broken and often deeply fractured, producing tor-like features, suggesting significant frost action (Hughes, 2002a). However, some areas of bedrock exhibit evidence of ice-scouring and perched boulders occur along the summit ridge. It is clear that ice has overridden the highest parts of Arenig Fawr at some point in the past. Hughes (2002a,b) argued that the temporal relationship between the ice-scouring and superficial frost weathering requires testing using cosmogenic exposure dating.

https://doi.org/10.1016/j.yqres.2015.11.003 Published online by Cambridge University Press

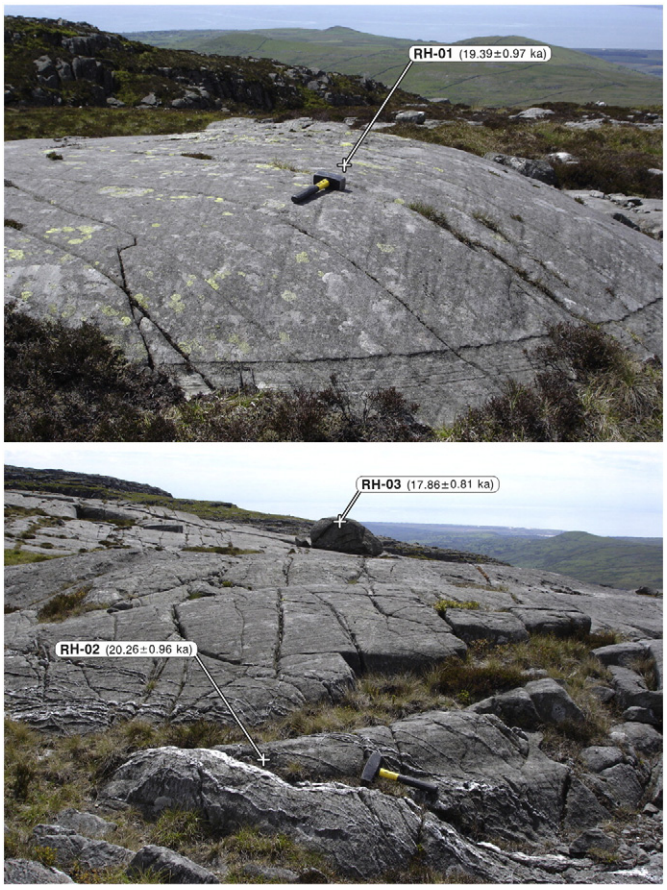

Figure 3. Sample sites in the Rhinogs. Photographs by Philip Hughes.

The evidence for ice overriding the summit of Arenig Fach is clearer than on Arenig Fawr. Several large (>1 × 1 × 1 m) perched subrounded and subangular boulders are present on the summit near the cairn of Carnedd y Bachgen. While these are locally-derived tuffs, they are clearly ice-transported. Perched boulders can be traced in a westerly direction from the summit cairn. Few perched boulders exist east of the summit cairn. This is consistent with ice movement from the west (to east) with boulders being dragged up the obstacle of Arenig Fach (in a similar way to the classic sites described by Darwin, 1848). Roches moutonnées, whalebacks and rock pavements are also present on the summit plateau of Arenig Fach and the entire summit area exhibits clear evidence of glaciation. The geomorphology of the lower slopes is also consistent with ice movement from west to east (Rowlands, 1979).

Geochronology

Geochronology — Rhinogs

Three samples were taken from the watershed of the northern Rhinogs between the peaks of Clip (598 m) and Moel Ysgyfarnogod (623 m). The first sample (RH01) was taken from a striated bedrock whaleback (Fig. 3) a short distance (~100 m) NE of Clip summit near Bwlch Gwylim. This sample gave an exposure age of 19.4 ± 0.7 ka (analytical error is used here and for each of the following dated samples). The second sample (RH02) was taken from a quartz vein on a striated rock pavement between Llyn Du and Moel Ysgyfarnogod (Fig. 3). This gave an exposure age of 20.3 ± 0.6 ka. The third sample (RH03) was taken from the top of a large subangular sandstone boulder (2.50 × 1.80 × 1.20 m) perched on a striated bedrock pavement of the same lithology. This sample is just 20 m to the south of the bedrock sample RH02 (Fig. 3) and yielded an exposure age of 17.9 ± 0.5 ka, 2 ka lower than the mean of RH-01 and -02. We note that this is the only erratic in the data set and also has the lowest exposure age when compared to the 19.3 ± 0.7 ka mean age from all the 8 bedrock samples.

Geochronology — Moelwyns

Three samples were taken from the Moelwyns for ^{10}Be analysis (Figs. 5 and 6). One sample was taken from a quartz vein in siltstone bedrock near the summit of Moelwyn Bach (MW-01) at an altitude of 700 m and yielded an exposure age of 19.5 ± 0.7 ka. Two samples were also taken from Craigysgafn. The first sample was taken (MW-02) from a prominent smooth and polished section of the quartz outcrop on the south side of this ridge (Fig. 6) at an altitude of 650 m on the ridge crest and gave an identical exposure age of 19.4 ± 0.6 ka. The second sample (MW-03) was taken from the higher part of this ridge, at an altitude of 670 m between the subsidiary summit of Craigysgafn (689 m) and the slope leading up to Moelwyn Mawr (770 m). This sample was taken from a quartz vein in ice-scoured rhyolite bedrock (Fig. 6) and yielded an exposure age of 19.5 ± 0.6 ka. The resultant mean age for this site is 19.5 ± 0.40 ka (using weighted mean and standard mean error).

Geochronology — Arenigs

Three samples were taken from the Arenigs for ^{10}Be analysis: two from Arenig Fach and one from Arenig Fawr (Fig. 8). On Arenig Fach, one sample was taken from a quartz vein in tuff bedrock 50 m SE of the summit cairn (ARENIG-01) at an altitude of 680 m. This sample yielded an exposure age of 18.4 ± 0.7 ka. Another sample (ARENIG-02) taken from a quartz vein on top of a bedrock whaleback NE of the summit cairn, at an altitude of 650 m, a short distance (~50 m) from the cliff edge, gave an exposure age of 18.0 ± 0.6 ka. On Arenig Fawr, a sample (ARENIG-03) from a quartz vein in bedrock tuff a short distance north of the summit yielded an exposure age of 19.4 ± 0.6 ka (Fig. 8). The resultant mean age for the two Arenig summits is 18.6 ± 0.7 ka (1σ).

Discussion

Ice-scoured bedrock and perched boulders on the summit areas of the northern Rhinogs, Moelwyns and Arenigs indicate that all three mountains were overridden by ice during the Pleistocene. This indicates that the Welsh Ice Cap exceeded the highest summits (854 m) by an undetermined margin. The geomorphological evidence from the Rhinogs, Moelwyns and Arenigs is consistent with Smith and George (1961) who argued that the surface of the last Welsh Ice Cap must have been at an altitude of least 915 m. Smith and George (1961) and later Rowlands (1979) argued that the ice divide must have been west of Arenig Fawr and Arenig Fach. Erratic boulders on the summits of the Arenigs are entirely of local origin and appear to have been transported short distances from west to east. Similarly, on the Rhinog watershed, perched boulders are all of local origin. Nevertheless, Rowlands (1979) correctly placed the ice divide just a few kilometers west of the Arenig watershed (see Fig. 1) since tills on the eastern flank of the Rhinogs do, however, contain clasts of Arenig origin (Foster, 1970b). This, and the clear evidence of ice-movement from east to west across the Rhinogs therefore support an ice divide in the Arenigs as suggested by Rowlands (1979).

Evidence of glacial erosion is most striking in the Rhinogs. The excellent preservation of striated ice-scoured bedrock is helped by the nature of the very resistant Cambrian sandstones in this area. In parts of the Moelwyns, such as on Craigysgafn, glacial erosional landforms are also very well preserved and again this is because of the very resistant rhyolite bedrock. In the Arenigs, glacial erosional features are less obvious, most probably related to the fact that the Arenigs are formed in volcanic

https://doi.org/10.1016/j.yqres.2015.11.003 Published online by Cambridge University Press

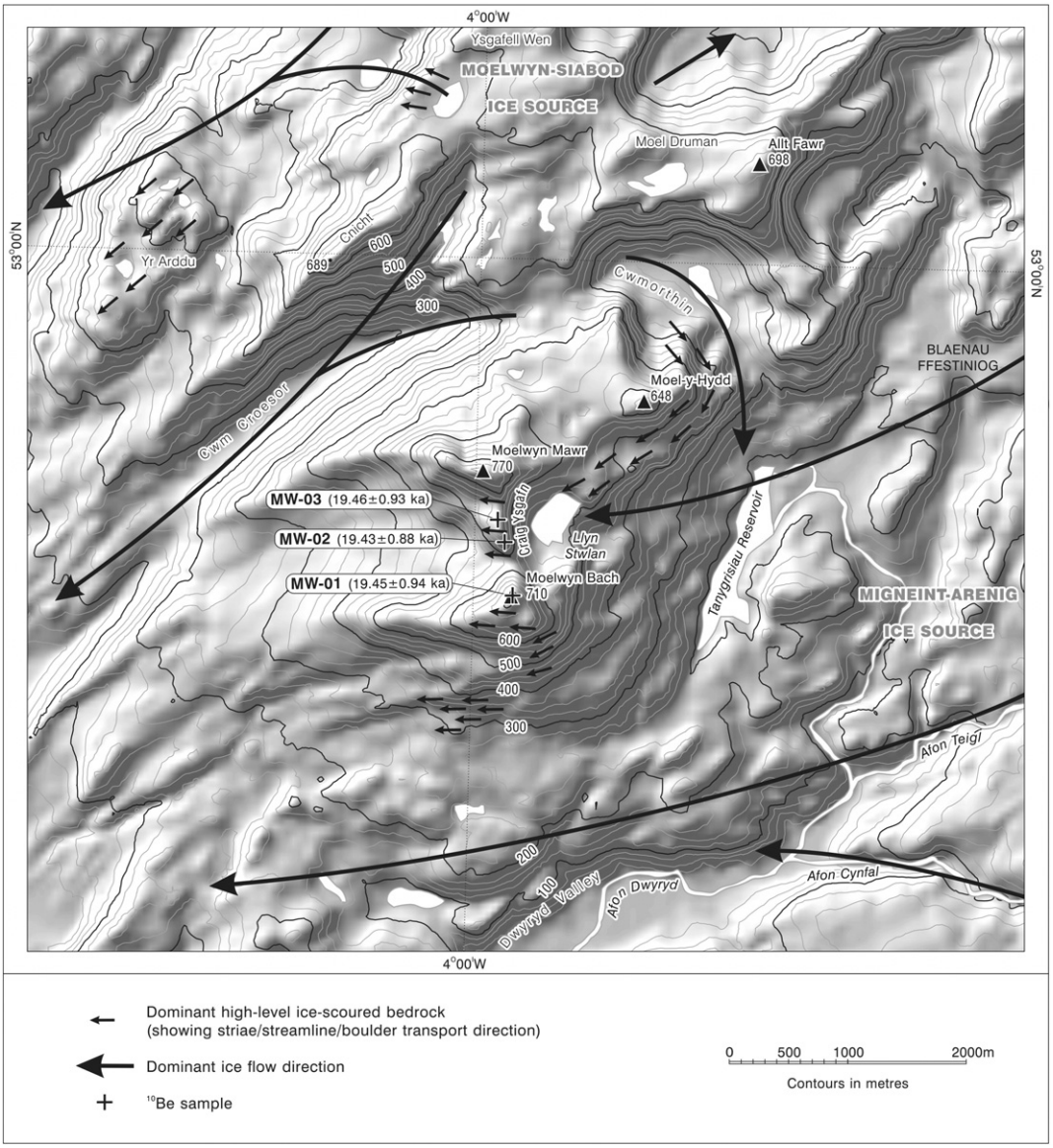

Figure 4. The Moelwyns showing the main ice flow directions and sample sites for ^{10}Be exposure dating. Location is marked on Figure 1.

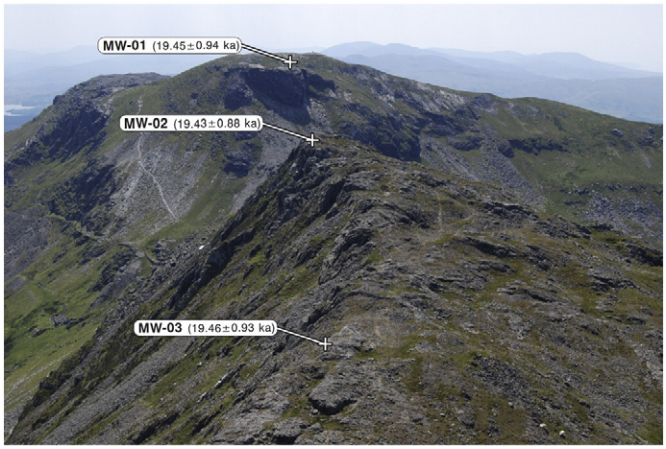

Figure 5. The Moelwyns showing the sample sites for ^{10}Be exposure dating. This photograph is taken from Moelwyn Mawr looking south over Craig Ysgafn and Moelwyn Bach. Sample site MW-02 is behind the summit of Craig Ysgafn. Photograph by Neil Glasser.

tuffs, which weather more easily than the very hard sandstone and rhyolite of the Rhinogs and Moelwyns. A few kilometers south-east of our sampled ranges, the nearby Arans are also formed in tuffs and as with the Arenigs, the glacial erosional landforms are not as clear as in the Rhinogs and Moelwyns. However, in addition to the lithological controls on glacial erosional landforms, the Arenigs and Arans were subject to slower ice velocities than the Rhinogs and Moelwyns during the maximum thickness of the last ice sheet (Patton et al., 2013b, their Fig. 8). Both the sampled areas of the Rhinogs and Moelwyns lay to the south-west and north-west of the ice divide, respectively, and both areas had elevated ice velocities with the greatest ice velocities occurring in the Dwyryd Valley that separates these two areas (Fig. 4).

All the new ^{10}Be ages reported in this work indicate that summits of the Rhinogs, Moelwyns and Arenigs emerged simultaneously through a decreasing ice cap thickness at c. 19.5 ka.. Mean exposure ages from the Rhinogs, Arenigs and Moelwyns overlap within their respective 1σ standard deviations (i.e. Rhinogs, 19.8 ± 0.6 ka ($n = 2$); Moelwyns, 19.5 ± 0.4 ka ($n = 3$); Arenigs, 18.6 ± 0.7 ka ($n = 3$)). The summit exposure ages from the Rhinogs, Moelwyns and Arenigs are very similar to those from the summit ridge of the Arans in southern Snowdonia

https://doi.org/10.1016/j.yqres.2015.11.003 Published online by Cambridge University Press

Figure 6. Close-up of sample sites in the Moelwyns. Photographs by Neil Glasser.

(Table 2) reported by Glasser et al. (2012) and re-calculated here using an identical procedure. The mean Aran exposure age of 19.41 ± 1.45 ka (7.5%, $n = 6$, 1σ) is indistinguishable from the combined mean bedrock ages from the Rhinogs, Moelwyns and Arenigs of 19.3 ± 0.7 ka (3.6%, $n = 8$, 1σ). As described in Glasser et al. (2012), we have also excluded two samples (AB-02, 36.2 ± 1.3 ka and AB-03, 29.3 ± 1.1 ka) which are clearly older outliers considered to have an inherited nuclide signal. The combined mean exposure age from all four areas (Rhinogs, Moelwyns, Arenigs and Arans) is 19.3 ± 1.0 ka ($n = 14$, analytical error only, 5.4% 1σ).

The highest bedrock samples from the new dataset obtained from the Rhinogs, Moelwyns and Arenigs, are from 824 m close to the summit of Arenig Fawr and from 700 m near the summit of Moelwyn Bach. These yielded exposure ages of 19.4 ± 0.6 ka (ARENIG-03), and 19.5 ± 0.7 ka (MW-01) while effectively identical exposure ages of 19.4 ± 0.7 ka and 20.3 ± 0.6 ka (RH-01 and RH-02) were obtained from the lowest bedrock samples at 581 and 589 m in the northern Rhinogs. The only boulder sampled yielded an exposure age that was about 1.5 ka younger (equivalent to 2σ) than the mean of all 8 of the bedrock samples.

This observation, although contingent on a single boulder age, may suggest the possibility that a portion of the cosmogenic nuclide inheritance signal of the order of 1–2 ka (i.e. 5%–10% of the measured exposure) persists in the bedrock samples. This can be readily seen as follows: if the most recent episode of sub glacial erosion during the LGM is required to fully remove an initial pre-LGM exposure of ~40 ka (derived from previous inter-glacials), uniform bedrock plucking of more than 300 cm would reduce it to <0.5 ka given a typical in-situ production half-length of ~40 cm. Lower and variable bedrock scouring of ~200 cm would raise this to 1.5 ka — equivalent to the differential noted above.

In order to assess if sub-glacial erosion was insufficient to fully remove inheritance, future sampling should target both bedrock and boulders, ideally as paired samples in close proximity. Given the problems of exhumation and toppling with boulder samples, in addition to the inheritance issues in bedrock, this would be the favored approach.

No clear trend appears between individual exposure ages and altitude from all 4 sites ($R^2 = 0.1719$). The exposure ages have a range of ~3.7 ka and are distributed over an altitude range of ~320 m. The highest bedrock samples from the new dataset obtained from the Rhinogs, Moelwyns and Arenigs, are from 824 m close to the summit of Arenig Fawr and from 700 m near the summit of Moelwyn Bach. These yielded exposure ages of 19.4 ± 0.6 ka (ARENIG-03), and 19.5 ± 0.7 ka (MW-01) while effectively identical bedrock exposure ages of 19.4 ± 0.7 ka and 20.3 ± 0.6 ka (RH-01 and RH-02) were obtained from the lowest bedrock samples at 581 and 589 m in the northern Rhinogs.

Essentially there is no clear difference in exposure ages over the altitudes of the summits sampled. Within the limits of the age resolution of our cosmogenic dating method, the exposure age results therefore clearly indicate a rapid decrease in the surface of the last Welsh Ice Cap of the order of ~300 m within a 1–2 ka time interval during the last termination (cf. Denton et al., 2010).

The exposure of the summits of the Welsh mountains at ~20–19 ka as the ice cap thinned is consistent with glaciological evidence from both Ireland and the Irish Sea to the west. In Ireland exposure ages from mountain summits, in a study similar to this one, indicate an early thinning of the last Irish Ice Sheet and emergence of high ground in Ireland at 24–21 ka (Ballantyne and Stone, 2015). Further east, the Irish Sea Ice Sheet expanded south into the Celtic Sea area between 34.0 and 25.3 ka, reaching maximum limits at 25.3–24.5 ka, based on several geochronological techniques (radiocarbon, cosmogenic isotope exposure ages and optically stimulated luminescence, see Chiverrell et al., 2013). The retreat of Irish Sea Ice Sheet exposing Holyhead Mountain in Anglesey, NW Wales had occurred by 18.8–21.4 ka (Chiverrell et al., 2013). All of this evidence is consistent with a maximum extent and thickness of both the Irish Sea Ice Stream and the adjacent Welsh Ice Cap during Greenland Stadial 3, which Hughes and Gibbard (2015) proposed is coeval with the global LGM. It is apparent that the thinning of the Welsh Ice Cap was synchronous with the retreat of the Irish Sea Ice Sheet and moreover, this process was rapid as shown by the new cosmogenic data presented in this paper.

Moraines of large valley glaciers are also present to the west of the Rhinogs (Foster, 1968, 1970a). The ages of these moraine systems are also unknown. Most attention has focused on the deglaciation history of the adjacent Irish Sea Ice Sheet (e.g. Brown et al., 1967; Foster, 1970a,b; Chiverrell et al., 2013). While a recent paper by Patton et al. (2013c) has investigated the geomorphological relationships between the Irish Sea Ice Stream and the adjacent Welsh Ice Cap, the timing of ice dynamics in the latter is still unresolved. Nevertheless, the new evidence from the mountain summits presented here helps to constrain

https://doi.org/10.1016/j.yqres.2015.11.003 Published online by Cambridge University Press

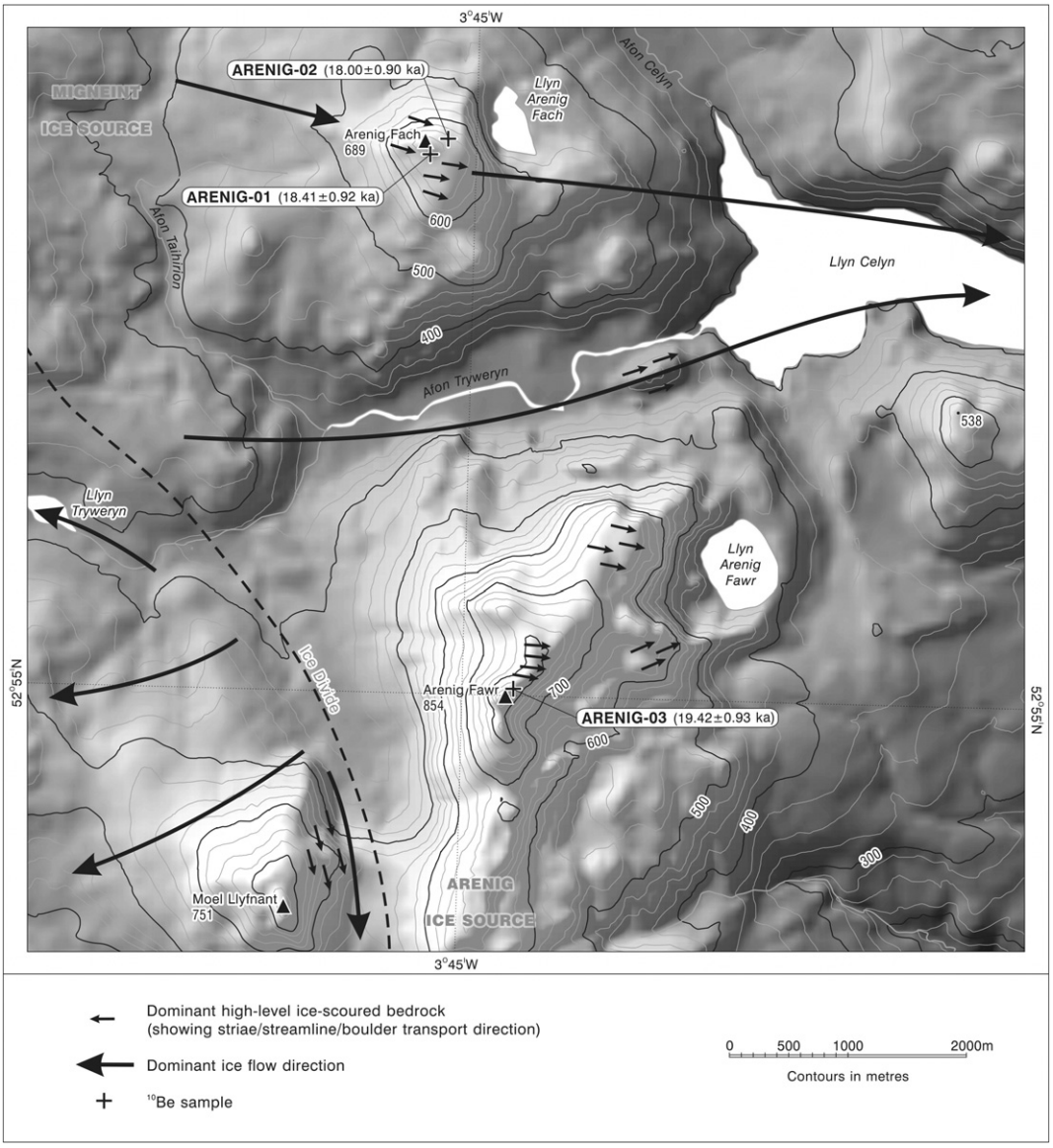

Figure 7. The Arenigs showing the main ice flow directions and sample sites for ^{10}Be exposure dating. The location of the ice divide is based on Rowlands (1979) as well as observations made in this paper. Location is marked on Figure 1.

the ages of Alpine-style valley glaciation in Wales. Based on the exposure ages from the watersheds presented in this study it is clear that the Welsh Ice Cap had thinned to below 600 m a.s.l. by 20–19 ka. Thus, the valley glacier moraines (which lie at altitudes from c. 400 m a.s.l. down to below sea level) mentioned above must post-date this period of ice cap retreat. This is important because it means that a period of glacier advance or stabilization occurred when the mountain peaks stood above as nunataks.

Radiocarbon dates from Llyn Gwernan on the northern side of the mountain Cadair Idris (892 m a.s.l.), a few kilometers to the south of the Rhinogs (see Fig. 1), indicate that valley glaciers had retreated in this area by 13.20 ± 0.12 ^{14}C ka BP (15.82 ± 0.39 cal. ka BP; calibrated using Calib 7.0, Reimer et al., 2013). All the mountain summits display evidence of periglacial weathering, superimposed onto the ice-scoured bedrock (Foster, 1970b; Hughes, 2002c; McCarroll and Ballantyne, 2002; Glasser et al., 2012) and this is consistent with a sustained period of intense periglacial activity on these summits after Late Pleistocene deglaciation. This means that there was potentially a period of c. 4 ka of Alpine-style valley glaciation, a time period more than three times as long as the Younger Dryas. This has important implications for the development of periglacial features that are present on the mountain summits of this study area. However, the age and history of the periglacial features found on the summits of higher summits in Snowdonia (Ball and Goodier, 1970; Addison, 1997; McCarroll and Ballantyne, 2000) remain an interesting question and further research is underway by the authors to examine the exposure history of the summits in the Snowdon and Glyder areas.

The last deglaciation history of the Welsh Ice Cap revealed in this paper has significant parallels with other ice masses around the North Atlantic where rapid retreat and thinning of ice masses occurred throughout the region soon after Heinrich Event 2. The Laurentide Ice Sheet in north-east America started retreating before 24 ka (Balco and Schäfer, 2006). In Norway, the Scandinavian Ice Sheet had begun retreating eastward depositing erratics on land by c. 20 ka (Svendsen et al., 2015). The onset of deglaciation before 20 ka around the margins of the North Atlantic suggests a common forcing that is most likely related to the changes in ocean–atmosphere interactions in this region. The combination of changing ocean conditions before, during and after Heinrich Event 2 (Gutjahr and Lippold, 2011) as well as a solar radiation peak at 24 ka (Alley et al., 2002) may have been responsible for large-scale ice sheet and ice cap instability on the Atlantic margins and triggered near-synchronous rapid deglaciation.

https://doi.org/10.1016/j.yqres.2015.11.003 Published online by Cambridge University Press

Figure 8. Sample sites in the Arenigs. Photographs by Philip Hughes.

Conclusions

The summits of the Rhinogs, Moelwyns and Arenigs in North Wales were covered by ice when the last Welsh Ice Cap was at its maximum and display evidence of ice scouring and transport of glacial boulders. The evidence is particularly pronounced in the Rhinogs and Moelwyns. Eight new ^{10}Be ages from ice-scoured bedrock and one from a perched boulder indicate that the mountain tops above ~600 m emerged above the ice cap by 19.5 ka, shortly after the LGM. Combined with a further six published ages from the Arans (Glasser et al., 2012; excluding two old outliers and recalculated here using a common method) there are now 15 ^{10}Be ages constraining the rate of vertical ice surface lowering of the last Welsh Ice Cap. The mean exposure age of all 14 bedrock samples (excluding the single erratic) is 19.3 ± 1.0 ka (n = 14, analytical error only, 5.4%, 1σ). These ages show that ice cap thinning was very rapid and exposure ages are statistically indistinguishable over a 320 m vertical range (581–901 m a.s.l.). This dataset is consistent with rapid thinning of ~300 m within a 1–2 ka period of the Welsh Ice Cap after the global Last Glacial Maximum (27.5 to 23.3 ka, based on the definition of Hughes and Gibbard, 2015) with the summits of the Rhinogs, Moelwyns, Arenigs and Arans all revealed more-or-less simultaneously as nunataks at c. 20–19 ka. The new insights into the timing of the vertical thinning of the last Welsh Ice Cap will help constraint numerical ice cap models and link in with evidence from the lateral margins (moraines, outwash, etc.) of the retreating ice cap. These findings from Wales accord with similar observations of former ice masses from the North Atlantic region. Large-scale ice sheet and ice cap instabilities around the North Atlantic margins are likely to have been triggered by changes in ocean circulation and solar forcing.

Acknowledgments

This research was funded by University of Manchester School of Environment, Education and Development Research Stimulation Fund. Laurence Totelin assisted in Moelwyns, Isabel Brown on Arenig Fach, and John Balfour, Mike Hambrey and Patrick Robson in the Rhinogs. We would also like to thank Stewart Campbell, Earth Science Officer at Natural Resources Wales, for his advice on permissions and protocols for working in the study areas. We acknowledge helpful and constructive comments from editor Alan Gillespie, associate editor Tom Lowell, an anonymous reviewer and Simon Cook. We would also like to thank Graham Bowden at the University of Manchester for drawing the figures.

References

Addison, K., 1997. Classic landforms of Snowdonia. Classic Landforms Guides. Geographical Association (60 pp.).
Alley, R.B., Brook, E.J., Anandakrishnan, S., 2002. A northern lead in orbital band: north–south phasing of Ice-Age events. Quaternary Science Reviews 21, 431–441.
Balco, G., 2011. Contributions and unrealized potential contributions of cosmogenic-nuclide exposure dating to glacier chronology, 1990–2010. Quaternary Science Reviews 30, 3–27.
Balco, G., Schäfer, J.M., 2006. Cosmogenic-nuclide and varve chronologies for the deglaciation of southern New England. Quaternary Geochronology 1, 15–28.
Balco, G., Stone, J., Lifton, N., Dunai, T., 2008. A complete and easily accessible means of calculating surface exposure ages or erosion rates from ^{10}Be and ^{26}Al measurements. Quaternary Geochronology 3, 174–195.
Ball, D.F., Goodier, R., 1970. Morphology and distribution of features resulting from frost-action in Snowdonia. Field Studies 3, 193–218.
Ballantyne, C.K., 2010. Extent and deglacial chronology of the last British-Irish Ice Sheet: implications of exposure dating using cosmogenic isotopes. Journal of Quaternary Science 25, 515–534.
Ballantyne, C.K., Stone, J.O., 2012. Did large ice caps persist on low ground in north-west Scotland during the Lateglacial Interstade? Journal of Quaternary Science 27, 297–306.
Ballantyne, C.K., Stone, J.O., 2015. Trimlines, blockfields and the vertical extent of the last ice sheet in southern Ireland. Boreas 44, 277–287.
Bendle, J.M., Glasser, N.F., 2012. Palaeoclimatic reconstruction from Lateglacial (Younger Dryas Chronozone) cirque glaciers in Snowdonia, North Wales. Proceedings of the Geologists' Association 123, 130–145.
Braucher, R., Bourles, D., Merchel, S., Vidal Romani, J., Fernadez-Mosquera, D., Marti, K., Léanni, L., Chauvet, F., Arnold, M., Aumaître, G., Keddadouche, K., 2013. Determination of muon attenuation lengths in depth profiles from in situ produced cosmogenic nuclides. Nuclear Instruments and Methods in Physics Research Section B: Beam Interactions with Materials and Atoms 294, 484–490.
Brown, M.J.F., Ellis-Gruffydd, I.D., Foster, H.D., Unwin, D.J., 1967. A new radiocarbon date for Wales. Nature 213, 1220–1221.
Child, D., Elliott, G., Misfud, C., Smith, A.M., Fink, D., 2000. Sample processing for Earth science studies at ANTARES. Nuclear Instruments and Methods B172, 856–860.
Chiverrell, R.C., Thrasher, I.M., Thomas, G.S.P., Lang, A., Scourse, J.D., van Landeghem, K.J.J., McCarroll, D., Clark, C.D., Cofaigh, Ó., Evans, D.J.A., Ballantyne, C.K., 2013. Bayesian modelling of the retreat of the Irish Sea Ice Stream. Journal of Quaternary Science 28, 200–209.
Chmeleff, J., von Blanckenburg, F., Kossert, K., Jakob, D., 2010. Determination of the ^{10}Be half-life by multicollector ICP-MS and liquid scintillation counting. Nuclear Instruments and Methods in Physics Research B 268, 192–199.
Clark, C.D., Hughes, A.L.C., Greenwood, S.L., Jordan, C., Sejrup, H.P., 2012. Pattern and timing of retreat of the last British-Irish Ice Sheet. Quaternary Science Reviews 44, 112–146.
Darwin, C., 1848. On the transportal of erratic boulders from a lower to a higher level. Quarterly Journal of the Geological Society 4, 315–323.

Denton, G.H., Anderson, R.F., Toggweiler, J.R., Edwards, R.L., Schaefer, J.M., Putnam, A.E., 2010. The last glacial termination. Science 328, 1652–1656.
Dielforder, A., Hetzel, R., 2014. The deglaciation history of the Simplon region (southern Swiss Alps) constrained by ^{10}Be exposure dating of ice-molded bedrock surfaces. Quaternary Science Reviews 84, 26–38.
Dunai, T.J., 2002. Influence of secular variation of the geomagnetic field on production rates of in situ produced cosmogenic nuclides. Earth and Planetary Science Letters 193, 197–212.
Everest, J.D., Bradwell, T., Stoker, M.S., Dewey, S., 2013. New age constraints for the maximum extent of the last British-Irish Ice Sheet (NW Sector). Journal of Quaternary Science 28, 2–7.
Fearnsides, W.G., 1905. On the geology of Arenig Fawr and Moel Llyfnant. Quarterly Journal of the Geological Society 61, 608–640.
Fink, D., Smith, A., 2007. An inter-comparison of ^{10}Be and ^{26}Al AMS reference standards and the ^{10}Be half-life. Nuclear Instruments and Methods B259, 600–609.
Fink, D., McKelvey, B., Hannan, D., Newsome, D., 2000. Cold rocks, hot sands: in-situ cosmogenic applications in Australia at ANTARES. Nuclear Instruments and Methods in Physics Research B172, 838–846.
Foster, H.D., 1968. The glaciation of the Harlech Dome. University College London (University of London).
Foster, H.D., 1970a. Sarn Badrig, a submarine moraine in Cardigan Bay, north Wales. Zeitschrift für Geomorphologie 14, 473–486.
Foster, H.D., 1970b. Establishing the age and geomorphological significance of sorted stone-stripes in the Rhinog Mountains, North Wales. Geografiska Annaler 52, 96–102.
EDINA Geology Digimap, 2014. British Geological Survey (BGS) Data. http://edina.ac.uk/digimap/index.shtml.
Glasser, N.F., Hughes, P.D., Fenton, C., Schnabel, C., Rother, H., 2012. ^{10}Be and ^{26}Al exposure-age dating of bedrock surfaces on the Aran ridge, Wales: evidence for a thick Welsh Ice Cap at the Last Glacial Maximum. Journal of Quaternary Science 27, 97–104.
Greenly, E., 1919. The geology of Anglesey. Memoirs of the Geological Survey of Great Britain. HMSO, London.
Gutjahr, M., Lippold, J., 2011. Early arrival of Southern Source Water in the deep North Atlantic prior to Heinrich event 2. Paleoceanography 26, PA2101. http://dx.doi.org/10.1029/2011PA002114.
Hughes, P.D., 2002a. Loch Lomond Stadial glaciers in the Aran and Arenig Mountains, North Wales, Great Britain. Geological Journal 37, 9–15.
Hughes, P.D., 2002b. Nunataks and the surface altitude of the last ice-sheet in southern Snowdonia, Wales. Quaternary Newsletter 97, 19–25.
Hughes, P.D., 2002c. Nunataks and the surface altitude of the last ice-sheet in southern Snowdonia, Wales: a reply to McCarroll and Ballantyne (2002). Quaternary Newsletter 98, 15–17.
Hughes, P.D., 2009. Loch Lomond Stadial (Younger Dryas) glaciers and climate in Wales. Geological Journal 44, 375–391.
Hughes, P.D., Gibbard, P.L., 2015. A stratigraphical basis for the Last Glacial Maximum (LGM). Quaternary International 383, 174–185.
Hughes, A.L.C., Greenwood, S.L., Clark, C.D., 2011. Dating constraints on the last British–Irish Ice Sheet: a map and database. Journal of Maps 2011, 156–183. http://dx.doi.org/10.4113/jom.2011.1145.
Jansson, K.N., Glasser, N.F., 2005. Palaeoglaciology of the Welsh sector of the British–Irish Ice Sheet. Journal of the Geological Society, London 162, 25–37.
Kohl, C.P., Nishiizumi, K., 1992. Chemical isolation of quartz for measurement of in situ-produced cosmogenic nuclides. Geochimica et Cosmochimica Acta 56, 3583–3587.
Korschinek, G., Bergmaier, A., Faestermann, T., Gerstmann, U.C., Knie, K., Rugel, G., Wallner, A., Dillmann, A., Dollinger, G., Liese von Gostomski, Ch., Kossert, K., Maiti, M., Poutivtsev, M., Remmert, A., 2010. A new value for the half-life of ^{10}Be by heavy-ion elastic recoil detection and liquid scintillation counting. Nuclear Instruments and Methods in Physics Research B 268, 187–191.
McCarroll, D., Ballantyne, C.K., 2000. The last ice sheet in Snowdonia. Journal of Quaternary Science 15, 765–778.
McCarroll, D., Ballantyne, C.K., 2002. Nunataks and the surface altitude of the last ice-sheet in southern Snowdonia, Wales: a comment on Hughes (2002). Quaternary Newsletter 98, 10–14.
McCormack, D.C., Brocklehurst, S.H., Irving, D.H.B., Fabel, D., 2011. Cosmogenic ^{10}Be insights into the extent and chronology of the last deglaciation in Wester Ross, northwest Scotland. Journal of Quaternary Science 26, 97–108.
Mifsud, C., Fujioka, T., Fink, D., 2013. Extraction and purification of quartz in rock using hot-phosphoric acid for in situ cosmogenic exposure dating. Nuclear Instruments and Methods B294, 203–207.
Patton, H., Hubbard, A., Glasser, N.F., Bradwell, T., Golledge, N.R., 2013a. The last Welsh Ice Cap: part I — modelling its evolution, sensitivity and associated climate. Boreas 42, 471–490.
Patton, H., Hubbard, A., Glasser, N.F., Bradwell, T., Golledge, N.R., 2013b. The last Welsh Ice Cap: part 2 — dynamics of a topographically controlled ice cap. Boreas 42, 491–510.
Patton, H., Hubbard, A., Bradwell, T., Glasser, N.F., Hambrey, M.J., Clark, C.D., 2013c. Rapid deglaciation: asynchronous retreat dynamics between the Irish Sea Ice Stream and terrestrial outlet glaciers. Earth Surface Dynamics 1, 53–65.
Reimer, P.J., Bard, E., Bayliss, A., Beck, J.W., Blackwell, P.G., Bronk Ramsey, C., Buck, C.E., Cheng, H., Edwards, R.L., Friedrich, M., Grootes, P.M., Guilderson, T.P., Haflidason, H., Hajdas, I., Hatté, C., Heaton, T.J., Hogg, A.G., Hughen, K.A., Kaiser, K.F., Kromer, B., Manning, S.W., Niu, M., Reimer, R.W., Richards, D.A., Scott, E.M., Southon, J.R., Turney, C.S.M., van der Plicht, J., 2013. IntCal13 and MARINE13 radiocarbon age calibration curves 0–50000 years cal BP. Radiocarbon 55 (4). http://dx.doi.org/10.2458/azu_js_rc.55.16947.
Rolfe, C.J., Hughes, P.D., Fenton, C.R., Schnabel, C., Xu, S., Brown, A.G., 2012. Paired ^{10}Be and ^{26}Al exposure ages from Lundy: new evidence for the extent and timing of Devensian glaciation in the southern British Isles. Quaternary Science Reviews 43, 61–73.
Rowlands, B.M., 1971. Radiocarbon evidence of the age of an Irish Sea Glaciation in the Vale of Clwyd. Nature 230, 9–11.
Rowlands, B.M., 1979. The Arenig region: a study in the Welsh Pleistocene. Cambria 6, 13–31.
Smith, B., George, T.N., 1961. North Wales. British Regional Geology, HMSO, London ,3rd Edition (96pp.).
Stone, J.O., 2000. Air pressure and cosmogenic isotope production. Journal of Geophysical Research-Solid Earth 105, 23753–23759.
Svendsen, J.I., Briner, J.P., Mangerud, J., Young, N.E., 2015. Early break-up of the Norwegian Channel Ice Stream during the Last Glacial Maximum. Quaternary Science Reviews 107, 231–242.
Thomas, G.S.P., Chiverrell, R.C., 2007. Structural and depositional evidence for repeated ice-marginal oscillation along the eastern margin of the Late Devensian Irish Sea Ice Stream. Quaternary Science Reviews 26, 2375–2405.
Travis, C.B., 1944. The glacial history of the Berwyn hills, North Wales. Proceedings of the Liverpool Geological Society 19, 14–28.
Whittow, J.B., Ball, D.F., 1970. North-west Wales. In: Lewis, C.A. (Ed.), The Glaciations of Wales and Adjoining Areas. Longman, London, pp. 21–58.

https://doi.org/10.1016/j.yqres.2015.11.003 Published online by Cambridge University Press